UC Santa Cruz
2010 International Summer Institute for Modeling in Astrophysics

Title
Thermohaline mixing with the small Peclet number approximation

Permalink
https://escholarship.org/uc/item/6t8022wn

Authors
Lagarde, Nadege
Lignieres, Francois
Zahn, Jean-Paul

Publication Date
2010-09-01

Thermohaline mixing in the small-Péclet number approximation.

Nadège Lagarde

in collaboration with François Lignières, and Jean-Paul Zahn

ISIMA 2010

- The International Summer Institute for Modeling in Astrophysics -

Abstract : Thermohaline mixing is the mechanism that governs the photospheric compostion of low- and intermediate-mass stars, and explain observations in these stars. It is important to study this instability with the hydrodynamic theory, and to derive prescriptions for the turbulent mixing that can be implemented in stellar codes. In this project, we discuss the formation of salt fingers on stable state, for different perturbations, when we use the small Péclet number approximation. The dominant mode of thermohaline mixing is different from the most unstable mode.

1   Introduction

Thermohaline mixing is well known in Oceans on Earth. In fact, the term thermohaline mixing refers to the part of the large-scale ocean circulation that is driven by global density gradients created by surface heat and cold water fluxes. The adjective thermohaline derives from thermo- referring to temperature and -haline referring to salt content, factors which together determine the density of sea water. In the polar regions (Arctic Ocean and Weddell Sea in particular), sea water turns into ice. Upon solidifying, the salts are rejected because the ice does not integrate them into its structure: liquid water is enriched in salts and the density increases, which begins a dive to the seabed and, eventually, large scale convection. So, this mixing is a double diffusive instability with two components : one stabilizing (temperature) diffuses faster than the other (Salt) whose stratification is unstable.

This instability has been already discussed in the literature : the first discussion by Stern (1960) ; Ulrich (1972) was the first to derive a prescription for this mehcanism ; Schmitt (1979) ; Kippenhahn et al. (1980) extended the Ulrich's prescription for the non-perfect gas, and Denissenkov (2010). In addition, in the laboratory, the instability takes the form of salt fingers (Krishnamurti 2003). Recently, thermohaline mixing has been identified as the mechanism that governs the photospheric composition of low- and intermediate mass stars (Charbonnel & Zahn 2007). In such stars, this double diffusive instability is induced by the inversion of mean molecular weight, created by the reaction $^3He(^3He, 2p)^4He$ on the external wing of the hydrgen burning shell. In fact, this mixing can explain observed abundances in the red giant stars (Charbonnel & Lagarde 2010).

In addition, this instability appears in various other astrophysical situations, for instance when ^4He or C-rich material is deposited at the surface of a star in a mass

transferring binary (Stothers & Simon 1969; Stancliffe et al. 2007), and when a star accretes heavy elements during planet formation (Vauclair 2004).

So it is very important to study this instability with the hydrodynamic theory, and to derive prescriptions for the turbulent mixing that can be implemented in stellar codes. As compared to oceans, a specificity of stellar fluid is its very high thermal diffusivity. This introduces scale separation effects that are difficult handle in numerical simulations. Here, we shall use the small-Pclet-approximation of the Boussinesq equations (Lignires 1999) that avoids this numerical difficulty but still enables to study the dynamics of an highly thermally diffusive atmosphere and in particular the thermohaline convection.

2 Equations for thermohaline instabilty with in small-Péclet number approximation

2.1 Boussinesq Equations with small-Péclet

We consider the Boussinesq equations for thermohaline instability :

$$\frac{\partial \vec{u}}{\partial t} + \vec{u}.\nabla \vec{u} = -\nabla p - \frac{\rho'}{\rho} g \vec{e}_z + \nu \nabla^2 \vec{u} \tag{1}$$

$$\frac{\partial \theta}{\partial t} + \vec{u}.\nabla \theta = K_T \nabla^2 \theta \tag{2}$$

$$\frac{\partial \mu}{\partial t} + \vec{u}.\nabla \mu = K_\mu \nabla^2 \mu \tag{3}$$

$$\vec{\nabla}.\vec{u} = 0 \tag{4}$$

where, $\vec{u} = u\vec{e}_x + v\vec{e}_y + w\vec{e}_z$ is the velocity vector, p the pressure, θ the temperature, and μ the mean molecular weight. The z axis refers to the vertical direction, while x and y axis are the horizontal directions. K_T and $K\mu$ correspond to the thermal and haline diffusivity respectively. The vertical velocity, temperature and salinity perturbations are of the form $e^{\lambda t} sin(m\pi z)e^{i(kx+ly)}$, where λ is the growth rate. We note the wave number $a^2 = k^2 + l^2 + m^2\pi^2$, and $a_h^2 = k^2 + l^2$ the horizontal wave number. We consider the linear case, $\vec{u}.\nabla \vec{u} = 0$.

In stars, the thermal diffusivity largely exceeds the viscosity and the haline diffusivity. So with the expression of Péclet number given by (Lignières 1999) and his discussion, we can take small Péclet number in stellar radiative zones. In addition, the equation of state is $\frac{\rho'}{\rho} = -\alpha\theta + \sigma\mu$, where $\alpha = \frac{1}{T}$ is the coefficient of thermal expansion in stars, and $\sigma = \frac{1}{\mu}$ the coefficient of haline contraction in stars. In the context of Boussinesq approximation, with the small-Péclet number approximation and using this equation of state, we obtain the following equations for thermohaline mixing.

$$(\lambda - \nu\nabla^2)\nabla^2 w = g(\alpha\nabla_h^2\theta - \sigma\nabla_h^2\mu) \tag{5}$$

$$K_T\nabla^2\theta = -\beta_T w \tag{6}$$

$$(\lambda - K_\mu\nabla^2)\mu = -\beta_\mu w \tag{7}$$

2

where $\beta_T = -\frac{\partial T}{\partial z}$ and $\beta_\mu = \frac{\partial \mu}{\partial z}$ are thermal and salinity gradients respectively. Substituting equations (6) and (7) in (5) gives the following quadratic equation for λ :

$$\lambda^2 + B\lambda + C = 0 \tag{8}$$

with

$$B = \frac{\hat{a}^2 \nu}{L^2}\left[1 + \frac{K_\mu}{\nu} + \frac{\hat{a}_h^2}{\hat{a}^6}Ra_T\right] \tag{9}$$

and

$$C = \frac{\hat{a}^4 \nu K_\mu}{L^4}\left[1 + \frac{\hat{a}_h^2}{\hat{a}^6}\left(Ra_T - Ra_\mu\right)\right] \tag{10}$$

where the wavenumbers have been non-dimensionalized

$$\hat{a} = aL \qquad \hat{a}_h = a_h L \tag{11}$$

and where we have introduced the thermal and haline Rayleigh numbers

$$Ra_T = -\frac{g\alpha\beta_T L^4}{\nu K_T} \qquad Ra_\mu = \frac{g\sigma\beta_\mu L^4}{\nu K_\mu}. \tag{12}$$

2.2 Study of stability

For $C < 0$ the discriminant $\Delta = B^2 - 4C$ is positive, thus the quadratic equation has two real roots, of which one is positive, leading to exponential growth. This root vanishes for $C = 0$, namely when

$$Ra_\mu - Ra_T = \frac{\hat{a}^6}{\hat{a}_h^2}. \tag{13}$$

The minimum of $(Ra_\mu - Ra_T)$ is obtained for $\hat{a}_h^2 = m^2\pi^2/2$, which yields the instability condition at small Péclet number :

$$Ra_\mu - Ra_T > \frac{27}{4}\pi^4. \tag{14}$$

One retrieves the familiar condition for thermal convection when one ignores Ra_μ and changes the sign of Ra_T (since then $\beta_T < 0$).

3 2D Simulations in the non-linear regime : the dominant mode

In order to explore the non-linear regime, and know the dominant mode of the thermohaline instability, we use the code Balaitous. It is a 3D code that uses a pseudo-spectral Fourier method in the horizontal directions and compact finite differences in the vertical. We compute two dimensions simulations, with 101x128 grid points. The vertical extend of the domain is L and the horizontal one is $2\pi L$. In the horizontal direction the boundary conditions are periodic. At the bottom and top surfaces, the velocity satisfies stress-free impenetrable boundary conditions while the perturbations of mean molecular weight and temperature vanish there.

The initial conditions are inspired from the solution of the linear equations (5)- (7) ; for the velocity components ($\hat{w}$ and $\hat{u}$), and the mean molecular weight ($\hat{\mu}$). We take respectively :

$$\hat{w} = \hat{w}_0 \sin(m\pi\hat{z})\cos(\hat{a}_h\hat{x}) \tag{15}$$

$$\hat{u} = -\frac{m}{2\hat{a}_h}\hat{w}_0 \cos(m\pi\hat{z})\sin(\hat{a}_h\hat{x}) \tag{16}$$

$$\hat{\mu} = \frac{-K_\mu}{\nu R_{a_T}}\hat{w}_0 \tag{17}$$

where $\hat{a}_h$ is an integer.

We take $R_{a_T} = 100$ and $R_{a_\mu} = 1000$. In these conditions, we find the most unstable mode for linear growth rate $a_h = 3.92$. In order to determine the dominant mode of thermohaline instability, we compute simulations with two perturbations which have two different horizontal wave numbers, and the same initial amplitude.

In table 1, we show the different models computed, with different horizontal wave numbers.

3.1 $a_h = 4$ and 2

Figure 1 shows the vertical velocity at $x = \frac{\pi}{4}$ as a function of time, for model computed with initial wavenumbers $a_h = 4$ and $a_h = 2$. The system tends towards a stable solution when $t = 30$. Figure 2 represents the mean molecular weight in grey, when the system is stable. The system tends directly towards a stable solution with the formation of two salt fingers. This fingers take the form of mushroom.
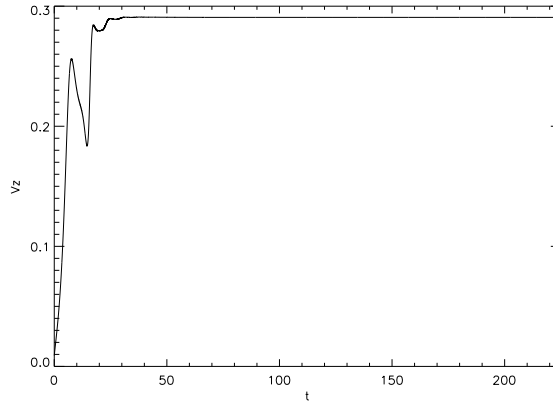

Figure 1: The vertical component of velocity as a function of time, for model with initial wavenumbers $a_h = 4$, $a_h = 2$.

3.2 $a_h = 4$ and 5

Figure 3 shows the vertical velocity at $x = \frac{\pi}{4}$ as a function of time, for model with initial wavenumbers $a_h = 4$ and $a_h = 5$. The system tends towards an intermediate solution when $t = 20$, and after a stable solution when $t > 200$.

Figure 4 represents the mean molecular weight in grey, when the system is in intermediate state (left panel) with four saltfingers, and stable state (right panel) with only two saltfingers.
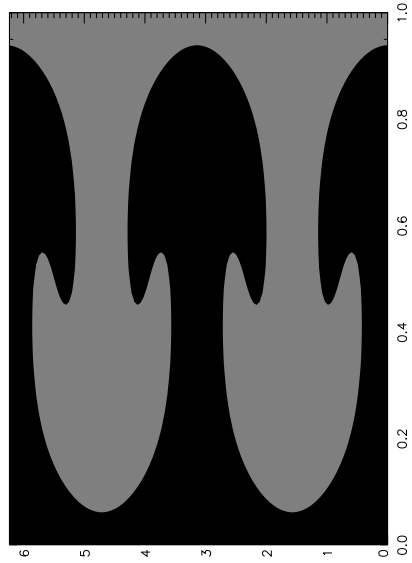
4

Figure 2: Salinity (in grey) at t=225, for model with initial wavenumbers $a_h = 4$, $a_h = 2$.
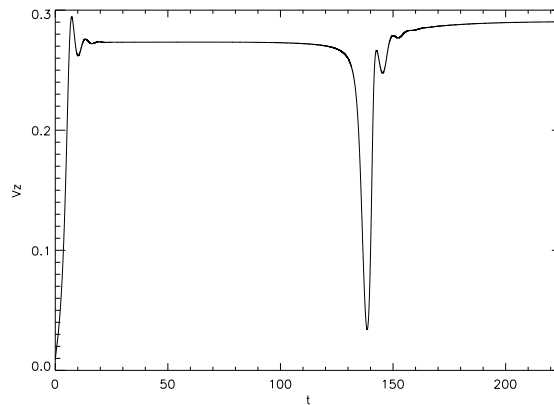

Figure 3: The vertical component of velocity as a function of time, for model with initial wavenumbers $a_h = 4$, $a_h = 5$.

3.3 $a_h = 5$ and 9

Figure 5 shows the vertical velocity at $x = \frac{\pi}{4}$ as a function of time. The system, as for previous model, tends towards an intermediate solution (t=20), and then into a stable solution (t ¿150). Figure 6 represents the mean molecular weight in grey, when the system is in intermediate state, and stable state respectively. The system forms five salt fingers on the intermediate state, and then three on stable solution.
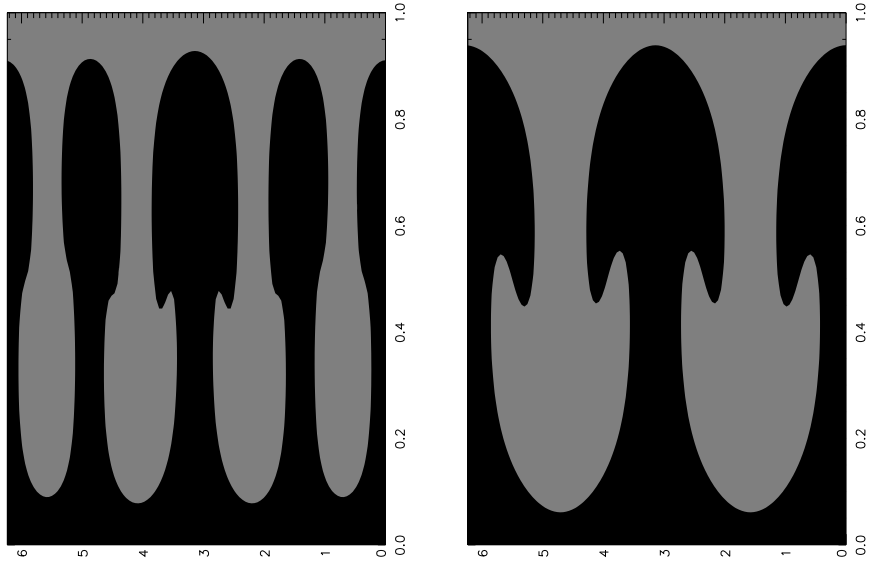
Figure 4: Salinity (in grey) at t=90s (left) and at t=225 (right), for model with initial wavenumbers $a_h = 4$, $a_h = 5$.
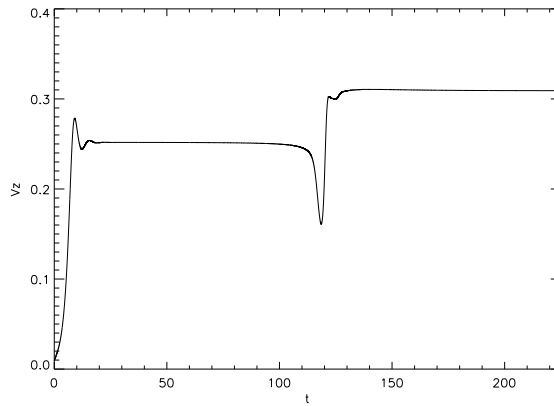

Figure 5: The vertical component of velocity as a function of time, for model with $a_h = 5$ $a_h = 9$.

4 Conclusions and future work

We applied the small-Péclet number approximation to the equations of thermohaline mixing. In these conditions, we have obtained a condition of thermohaline instablity, linked directly with the thermal and haline Rayleigh numbers. Then we have computed nine models with two perturbations which have two different horizontal wave numbers, in order to determine the dominant mode. We have shown that the dominant mode is different from the most unstable mode.
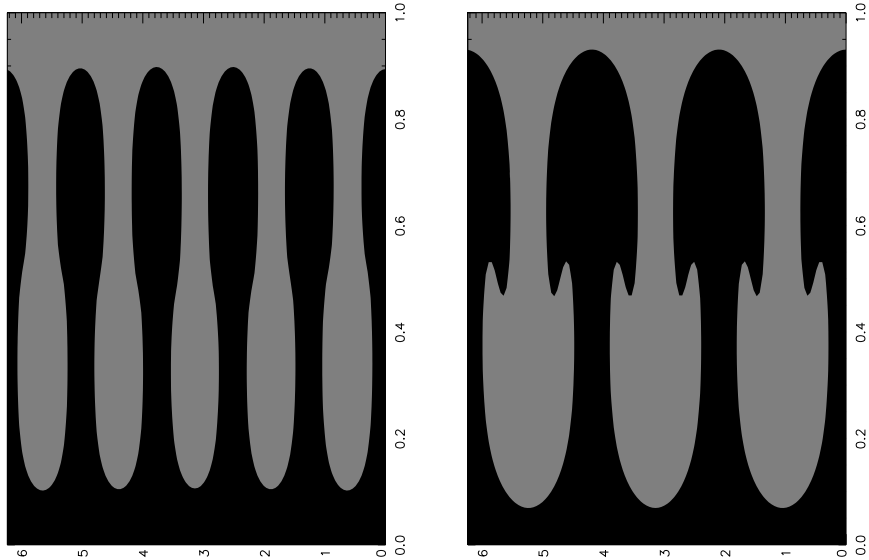
6

Figure 6: Salinity (in grey) at t=90s (left) and at t=225 (right), for model with $a_h = 4$ $a_h = 5$.

For all our models, the system tends towards a stable solution with two or three salt fingers. In addition, the table 1 shows two different evolutions. First, when the horizontal wave number is lower than the most unstable mode, the system tends directly to the stable mode. Second, when the horizontal wave number is higher than the most unstable mode, the system evolves to an intermediate state, and then to the final stable state.

The dominant mode of thermohaline mixing, in these conditions, is different from the most unstable mode.

In addition, we can study the aspect ratio of salt fingers. It is defined as the ratio between the length and width of fingers. In our conditions of computation, we obtain an aspect ratio equal to the normalized horizontal wavenumber. And we have seen that a_h is always superior to 1. In fact, the efficiency of mixing depends sensitively on this aspect ratio. The diffusive coefficient is given with the equation 18, where α is the aspect ratio of salt fingers, according to Ulrich (1972) :

$$D_t = \frac{8}{3}\pi^2\alpha^2 K(\frac{\phi}{\delta})\frac{-\nabla_\mu}{(\nabla_{ad} - \nabla)} \tag{18}$$

In future work, we must computed other simulations with different parameters in order to understand the effects on aspect ratio of salt fingers, and thus on the efficiency of thermohaline mixing, with two and three dimensions simulations

References

Charbonnel, C. & Lagarde, N. 2010, ArXiv e-prints

Models	a_h		intermediate state	stable state
M1	2	4	-	2
M2	2	6	-	2
M3	3	5	-	3
M4	3	6	-	3
M5	4	5	4	2
M6	5	8	5	3
M7	5	9	5	3
M8	6	10	6	2
M9	7	9	7	3

Table 1: Models computed with two different initial horizontal wave numbers (given in second column). The third and fourth columns give the number of saltfingers in the computational domain

Charbonnel, C. & Zahn, J.-P. 2007, A&A, 467, L15

Denissenkov, P. A. 2010, ArXiv e-prints

Kippenhahn, R., Ruschenplatt, G., & Thomas, H.-C. 1980, A&A, 91, 175

Krishnamurti, R. 2003, Journal of Fluid Mechanics, 483, 287

Lignières, F. 1999, A&A, 348, 933

Schmitt, R. 1979, Deep Sea Research Part I: Oceanographic Research, 26, 23

Stancliffe, R. J., Glebbeek, E., Izzard, R. G., & Pols, O. R. 2007, A&A, 464, L57

Stern, M. E. 1960, Tellus, 12, 172

Stothers, R. & Simon, N. R. 1969, ApJ, 157, 673

Ulrich, R. K. 1972, ApJ, 172, 165

Vauclair, S. 2004, in IAU Symposium, Vol. 224, The A-Star Puzzle, ed. J. Zverko, J. Ziznovsky, S. J. Adelman, & W. W. Weiss, 161–166